Inelastic Atom−Surface Scattering by Phonons: A Comparison of Different Approaches†

W. Brenig* and B. Gumhalter‡

Physik-Department, Technische Universität München, D-85747 Garching, Germany

Received: February 19, 2004; In Final Form: June 9, 2004

The inelastic scattering of atoms by phonons of a semi-infinite solid involves infinitely many degrees of freedom and hence cannot be treated rigorously by any of the known numerical methods. An approximation which has been used successfully to explain experimental data is the exponentiated Born approximation (EBA). Here we compare this approximation for the scattering by an Einstein-model with two types of coherent state approximations (where the wave function is approximated by a Gaussian centered at the classical trajectory) and with the results of an exact coupled channel calculation. The EBA turns out to be close to the coherent state approximations, and all three agree rather well with the exact results except near thresholds and (in particular) resonances. The calculations are done for zero temperature *T* but excited initial states are considered from which nonzero *T* results can be obtained as Boltzmann averages.

I. Introduction

The quantum mechanical treatment of atom−surface scattering, historically, goes back to the 1930s when it emerged as one of the first problems to be attacked by theoretical surface physics.[1] Naturally, the problem of inelastic atom scattering by phonons could only be treated approximately, for instance by resorting to what is now called the distorted wave Born approximation (DWBA).[2,3] This treatment was later taken up again to describe accommodation and sticking processes mediated by phonons.[4] In ref 4, some deficiencies of the DWBA were pointed out and partially remedied.

For low energy scattering of light particles by heavy substrate atoms, the DWBA works reasonably well. In this case, the fraction of elastically scattered particles, expressed through the so-called Debye−Waller factor (DWF), is large and the number of substrate phonons excited in the collision is small. However, with increasing energy and mass of the scattered particles, the DWF decreases and the number of excited phonons increases. If the number of excited phonons becomes larger than unity, the DWBA breaks down. A straightforward way to improve this situation is, of course, to go to higher orders in the Born expansion. This approach has been followed by Armand et al.[5] If the number of excited phonons is, say, *n*, one then has to go at least to *n*th order in the perturbation expansion. This becomes increasingly cumbersome and hence cannot be carried out without introducing further approximations. Furthermore, the unitarity of the scattering matrix is strongly violated if one straightforwardly truncates its perturbation expansion beyond the *n*th term. The unitarity of the scattering matrix is crucial for a correct value of the DWF, in particular if the number of excited phonons is large and hence the DWF small.

A fully unitary approximation for calculating the atom-phonon scattering amplitudes is based on the observation that the problem of a harmonic quantum oscillator linearly perturbed by a *classical* force $F(t)$ can be treated exactly.[6−12] This so-called forced oscillator model (FOM) was used to treat the scattering of He atoms by phonons of a Debye solid.[13,14] The force was in this case calculated from the classical trajectory of the corresponding classical scattering problem. In such a treatment, the quantum effects associated with the *substrate phonons* are properly taken into account: there is a nonzero elastic scattering probability, as measured by the DWF, and a suppression of the low energy sticking probability for light scattered particles.[15] Furthermore, the total scattering probability is equal to unity as required by the unitarity of the scattering operator. For large inelasticity (i.e. small DWF) this is a great advantage as compared to low order perturbation theory. On the other hand, the quantum effects associated with the motion of the *scattered particle* are completely neglected in this approach. Thus, for instance, the threshold behavior of the scattering cross sections (and hence their low energy limit[16]) is not described properly. Also, the existence of scattering resonances due to the bound states of the static projectile-surface is beyond the scope of classical treatments.

A step toward a full quantum treatment was made by invoking the eikonal approximation (EA)[17−20] to calculate the scattering probabilities. Like in the FOM, the scattering probabilities obtained in the EA satisfy unitarity and in addition this treatment gives also a hint for introducing quantum improvements concerning the motion of the scattered particle at least at higher energies. However, as the EA is essentially a single hit approximation, it cannot account for multiple scattering processes leading to resonance effects[21−23] that are important for a correct quantum interpretation of the interplay between bound state resonances and inelastic scattering phenomena.

A quantum mechanical generalization of the FOM can be derived[24] and most easily carried out in the so-called "exponentiated Born approximation"[25] (EBA). In the EBA the Fourier transform $F(\omega)$ of the force $F(t)$ in the expression for the transition probabilities is replaced by the corresponding matrix element of the quantum mechanical force acting on the projectile atom, calculated between the states describing unperturbed atom motion in the surface potential. As a consequence, the threshold behavior of the single phonon scattering probabilities is correctly described: below the threshold the probability vanishes and just above the threshold energy E_s one finds the correct behavior $\propto(E - E_s)^{1/2}$. Consequently, the low energy limit of sticking probabilities is also properly described in this approximation.

† Part of the special issue "Gerhard Ertl Festschrift".

* To whom correspondence should be addressed.

‡ Permanent address: Institute of Physics, P.O. Box 304, 10000 Zagreb, Croatia. E-mail: branko@ifs.hr.

10.1021/jp040151e CCC: $27.50
Published on Web 09/16/2004

However, although the EBA takes into account the quantum effects associated with both the phonons and projectile dynamics to a large extent, and the unitarity is properly fulfilled, it is still an approximation. Indeed, it can be shown[11,25,26] that the EBA can be obtained as the lowest order (unitary) term of a cumulant expansion to an exact expression for the scattering operator *S*. Similar expressions have been successfully applied before to electronic problems.[27]

The EBA expressions for the energy distribution of the scattered particles[24] and the full angular resolved scattering spectrum,[11,19,26] which include multiphonon and quantum effects in the coupled system, have been successfully applied in the interpretation of many experiments, mainly involving thermal energy noble gas atom scattering from surfaces,[11] adsorption,[28] and accommodation[29] and in particular He atom scattering (HAS) from phonons of the various adsorbed layers.[30−32]

Although the EBA results for the inelastic scattering probabilities are usually in a very good accord with the experimental data, the question of the validity of this approximation and how to improve it is still of major importance. This is due to the nondiminishing demand for reliable interpretation of the experimental data on inelastic atom−surface scattering that continue to reveal novel or controversial properties of surface vibrations.[33] Three different routes of the assessment of the EBA have been followed in the literature. The first one extends the first-order Born approximation in the EBA by inclusion of higher order terms in the cumulant expansion of the scattering matrix, but this method[11] proves rather cumbersome.

The second route goes back in some sense to the trajectory treatment and the FOM described above: The wave function of the FOM corresponds to the ground state of a displaced oscillator.[6,9] The displacement of the coordinate (described by a shift in coordinate space) and momentum (described by the corresponding phase factor) are calculated from the classical trajectory of the model. On top of this displaced ground-state wave function, one then considers the complete orthonormal system of *displaced excited* oscillator states and uses this as a basis for a coupled channel treatment of the scattering problem. By taking sufficiently many excited states into account this allows a virtually exact numerical solution of the problem, just as in the general coupled channel method. Moreover, using the displaced basis states the ground-state already takes the classical part of the scattering problem into account. One can hope, therefore, that the displaced basis is *optimized* in the sense that fewer channels are needed in the coupled channel treatment. This has indeed been shown to be true[34] and could be used for a coupled channel treatment of a 7D problem in surface physics.[35]

The third possibility to *check* the validity of the EBA is to consider simple models which can be solved exactly (for instance numerically) and to compare the exact results with those of the various approximations. The first step in this direction was taken some time ago in the calculations of temperature dependence of the Debye−Waller factor.[36] More recently, the energy dependence of the various transition probabilities was considered in a similar fashion and special emphasis was put on the effects of nonlinear projectile-phonon coupling.[37] There, to avoid the problems with bound state resonances, only the purely repulsive projectile−surface potentials were considered. In this paper, we extend the treatment of the energy dependence of inelastic scattering probabilities to the potentials with attractive wells. Then the main difference between the simple EBA and exact results is the occurrence of strong resonance structures at low energies (below 10 meV).

II. Two-Dimensional Model for Inelastic Particle Scattering from a Surface Oscillator

The two-dimensional (2D) model which we shall use in our studies is the same one as in refs 36 and 37: it is appropriate to describe He atom scattering from vibrating noble gas adsorbates weakly bound to planar crystal surfaces, typically Xe adsorbed on Cu or graphite. The scattered atoms couple most strongly to the vertically polarized adsorbate phonons which show little dispersion and therefore can be accuratly described by an Einstein model in which the oscillator frequency ω is constant. The Hamiltonian of the system, expressed in terms of the projectile and oscillator coordinates and the conjugate momenta, (z, q) and (x, p), respectively, then takes the form

$$H = \frac{p^2}{2M} + \frac{q^2}{2m} + \frac{M}{2}w^2x^2 + v(z-x) \tag{1}$$

where M and m are the oscillator and projectile atom mass, respectively. We model the He−Xe interaction by a Morse potential

$$v(z-x) = D(e^{-2\alpha(z-x)} - 2e^{-\alpha(z-x)}) \tag{2}$$

where α and D denote the inverse range and the well depth of the potential, respectively. The scattering system He → Xe/Cu has been investigated extensively, both experimentally[30] and theoretically,[11] and hence may be used as a useful and simple testing ground for applications of the various theoretical methods. The parameters appropriate to the He → Xe/Cu system are (m_p is the proton mass)

$$m = 4m_p;\ M = 131m_p;\ \hbar\omega = 2.7\ \text{meV};$$
$$\alpha = 1.22\ \text{Å}^{-1};\ D = 6.6\ \text{meV} \tag{3}$$

Together with the potential $v(z-x)$ we introduce the force acting on the projectile atom

$$f(z-x) = -\frac{\partial}{\partial z}v(z-x) \tag{4}$$

Then the Heisenberg equations of motion for $p(t)$, $x(t)$, $q(t)$, and $z(t)$ take the form

$$M\frac{dx}{dt} = p,\ \frac{dp}{dt} = -M\omega^2x + f(z-x) \tag{5}$$

and

$$m\frac{dz}{dt} = q,\ \frac{dq}{dt} = -f(z-x) \tag{6}$$

The first two equations (for the oscillator) can be combined into a single one. By introducing the annihilation and creation operators (in the Heisenberg picture) for the oscillator quanta, respectively, by the expressions

$$b(t) = [M\omega x(t) + ip(t)]/(2M\hbar\omega)^{1/2} \tag{7}$$

$$b^\dagger(t) = [M\omega x(t) - ip(t)]/(2M\hbar\omega)^{1/2} \tag{8}$$

we find the Heisenberg equation of motion for the annihilation operator

$$[\omega - i(d/dt)]b(t) = \frac{f(z(t)-x(t))}{(2M\hbar\omega)^{1/2}} = \frac{x_0}{\hbar}f(z(t) - x_0[b(t) + b^\dagger(t)]) \tag{9}$$

where $x_0 = (\hbar/2M\omega)^{1/2}$ is the root-mean-square displacement of the oscillator. The corresponding equation of motion for $b^\dagger(t)$ is obtained by hermitian conjugation of (9).

The scattering states with incoming initial ($-q_i$) and outgoing final (q_f) momenta of the scattered particle and initial (m), final (n) quantum numbers of the oscillator can be defined as

$$|m,q_i\rangle_{in} = \lim_{t\to-\infty} e^{i(H-E_i)t}|m\rangle|q_i\rangle_{in} \tag{10}$$

and similarly

$$|n,q_f\rangle_{out} = \lim_{t\to\infty} e^{i(H-E_f)t}|n\rangle|q_f\rangle_{out} \tag{11}$$

where $|q_i\rangle_{in}$ and $|q_f\rangle_{out}$ are the corresponding (elastic) scattering states of the Morse potential $v(z)$ alone, and $|m\rangle$ and $|n\rangle$ are the eigenstates of the unperturbed oscillator. The (total) energies $E_{i,f}$ in this equations are given by

$$E_i = \frac{q_i^2}{2m} + \hbar\omega(m + 1/2),\ E_f = \frac{q_f^2}{2m} + \hbar\omega(n + 1/2) \tag{12}$$

As is well-known, there exists a unitary operator S which transforms the "out" states into the "in" states. The matrix elements of this operator form the so-called S matrix

$${}_{out}\langle n,q_f|m,q_i\rangle_{in} = S_{n,m}(E)\delta(E_f - E_i) \tag{13}$$

where $E = E_i(= E_f)$ is the constant total energy of the scattering process.

Parallel to the "in" and "out" *states* it is useful to define corresponding boson field *operators* by

$$b_{out,in} = \lim_{t\to\pm\infty} b(t)e^{i\omega t} \tag{14}$$

where

$$b(t) = e^{iHt}be^{-iHt} \tag{15}$$

and b and $b^\dagger$ are the standard boson annihilation and creation operators for the unperturbed oscillator that are defined by

$$b|n\rangle = \sqrt{n}|n-1\rangle \tag{16}$$

From this definition and eqs 10, 11, and 13, it follows that the $b_{in,out}$ annihilate perturbed phonon quanta just as the b annihilate unperturbed phonon quanta, viz.

$$b_{out,in}|n,q_{f,i}\rangle_{out,in} = \sqrt{n}|n-1,q_{f,i}\rangle_{out,in} \tag{17}$$

Furthermore, the S operator transforms the "in" operators into the "out" operators:

$$b_{out} = S^\dagger b_{in} S \tag{18}$$

The last three equations have to be supplemented by the corresponding ones for the hermitean conjugate (creation) operators.

Another relation between b_{out} and b_{in} is obtained by integrating the Heisenberg equation of motion (9), which yields an integral equation for b_{out}

$$b_{out} = b_{in} + \int_{-\infty}^{\infty} e^{i\omega t}\frac{x_0}{\hbar} f(z(t) - x_0[b(t) + b^\dagger(t)])\,dt \tag{19}$$

with the scattering boundary condition

$$b_{in} = b \tag{20}$$

A completely analogous equation is obtained for $b_{out}^\dagger$.

We now use eqs 18 and 19 to discuss the three approximate treatments of the scattering problem: the forced oscillator approximation (FOA), the semiclassical (SEC), and the exponentiated Born approximation (EBA). All of these approximations agree on replacing the r.h.s of (19) by a complex number (instead of an operator). The two operators b_{out} and b_{in} then differ by a number which describes a shift of the "out" state relative to the "in" state in the corresponding phase space, but leaves its shape unchanged: the oscillator states are transformed into *displaced* oscillator states. Such states are usually called *coherent states*.

III. Approximate Treatments

A. Forced Oscillator Model. Underlying all three abovementioned approximations is the forced oscillator model (FOM), which can be solved exactly.[6−12] In the FOM, the quantum mechanical operator $f(t)$ on the rhs of (9) is replaced by a fixed classical force $F(t)$ that perturbs the oscillator. Then, eq 19 can be written as

$$b_{out} = b_{in} + B = b_{in} + \frac{x_0}{\hbar}F(\omega) \tag{21}$$

where $F(\omega)$ is the Fourier transform of the force $F(t)$:

$$F(\omega) = \int_{-\infty}^{\infty} dt\, e^{i\omega t} F(t) \tag{22}$$

Hence the classical force $F(t)$ gives rise to a displacement of the operator b_{in} by a classical quantity, i.e., a complex number B. Starting from the ground state with $b_{in}|0\rangle = 0$ this leads to a shift in the energy of the oscillator to

$$E_{osc} = \hbar\omega\langle b_{out}^\dagger b_{out}\rangle = \frac{|F(\omega)|^2}{2M} \tag{23}$$

which is well-known also from classical physics.

Equation 21 implies that there exists a unitary operator S in the form

$$S = e^{(Bb^\dagger - B^\dagger b)} = e^{-|B|^2/2}e^{Bb^\dagger}e^{-B^\dagger b} \tag{24}$$

such that (18) is valid. Hence, in this case, the displacement operator S can be identified as the scattering operator.

It is particularly simple to obtain the matrix elements $S_{n,0}$ for the transitions from the ground state. Since for the ground state $|0\rangle$ one has $b|0\rangle = 0$, one obtains

$$S|0\rangle = e^{-|B|^2/2}\sum_{n=0}^{\infty}\frac{B^n}{\sqrt{n!}}|n\rangle \tag{25}$$

where

$$B = \frac{x_0}{\hbar}F(\omega) \tag{26}$$

Therefore, $S_{n,0} = B^n \exp(-|B|^2/2)/\sqrt{n!}$, and for the transition probabilities one finds the well-known Poisson distribution

$$P_{n,0} = |S_{n,0}|^2 = \frac{N^n}{n!}e^{-N},\ N = |B|^2 \tag{27}$$

In particular, one finds for the Debye−Waller factor $P_{0,0}$

$$P_{0,0} = \mathrm{e}^{-N} \tag{28}$$

with the Debye−Waller exponent given by $N = |B|^2 = E_{\mathrm{osc}}/\hbar\omega$.

One also easily checks the unitarity of the transition probabilities

$$\sum_{n=0}^{\infty} P_{n,0} = 1 \tag{29}$$

and the expression for the mean number of excited oscillator quanta

$$\langle n \rangle = \sum_{n=0}^{\infty} n\, P_{n,0} = N \tag{30}$$

Hence, in the FOM the classical energy transfer to the oscillator measured in units of the oscillator energy quantum is equal to the average number of excited phonons.

In a similar way, one can derive from (24) the transition probabilities from an excited state[6−9,12]

$$P_{n,m} = |S_{n,m}|^2 = n!m!N^{(n-m)}\mathrm{e}^{-N}\left[\sum_{l=0}^{m}\frac{(-N)^l}{l!(n-m+l)!(m-l)!}\right]^2,\ n \geq m \tag{31}$$

which can be expressed also in terms of Laguerre polynomials. The values for $m \geq n$ can be obtained from (31) by interchanging m and n.

For the sake of completeness, we mention that the energy transfer starting from an excited state $|m\rangle$

$$\Delta E_m = \hbar\omega \sum_n (n-m) P_{n,m} = E_{\mathrm{osc}} \tag{32}$$

is independent of m and equal to E_{osc} in expression (23).

B. Forced Oscillator Approximation. For the scattering of a particle by an oscillator, there is no "fixed" force but if one treats the scattered particle classically and neglects the recoil effects in the force [i.e., the operator $x(t)$ in $f(z(t) - x(t))$ on the rhs of (19)] one can determine the classical trajectory $Z(t)$ of the scattered particle independently of the motion of the oscillator (from now on we denote classical quantities $Z(t)$ and $Q(t)$ by capital letters in contrast to the corresponding quantum operators $z(t)$ and $q(t)$). Then the resulting classical force $f(Z(t))$ can be used as an input in (21). It is fixed in the sense that it is independent of the motion of the oscillator. In contrast to the FOM, it depends on the initial energy E of the particle: $f(Z(t)) = F(t, E)$. We call the corresponding approximation the *FO* approximation (FOA). The neglect of recoil terms works reasonably well for He scattered by a Debye solid[38] and allows one to take into account quantum effects of the scattered particle in a simple, though approximate way, as we shall show later on. In this context we define

$$f(Z(t)) = F(t,E) \tag{33}$$

$$F(\omega,E) = \int_{-\infty}^{\infty} \mathrm{e}^{i\omega t} F(t,E)\, \mathrm{d}t \tag{34}$$

Inserting this into the rhs of (21), one finds the phase space displacement B of the FOA

$$B = F(\omega,E)/(2M\hbar\omega)^{1/2} \tag{35}$$

This is the approximation which was used in ref 13 to describe inelastic He-atom scattering by phonons.

The FOA can be improved without leaving the framework of coherent states in two ways: In the *semiclassical approximation* (SEC) one takes the recoil terms into account, but leaves the rhs of (19) classical. One then has to treat the coupled eqs. of motion for $X(t)$, $P(t)$, $Z(t)$, $Q(t)$ classically. Again we denote the average momenta, coordinates, etc. by capital letters, in particular we use use $B(t) = \langle b(t) \rangle$.

Let us begin with a situation in which the oscillator is initially in its ground state, then $B_{in} = 0$. Let us denote B_{out} by B and recall the definitions (7) and (14). Then the classical counterpart of expression on the r.h.s of (19) reads

$$B = \lim_{t\to\infty} \frac{[\omega X(t) + iP(t)]}{(2M\hbar\omega)^{1/2}}\mathrm{e}^{i\omega t} = \int_{-\infty}^{\infty} \mathrm{e}^{i\omega t}\frac{f(Z(t) - X(t))}{(2M\hbar\omega)^{1/2}}\,\mathrm{d}t \tag{36}$$

The quantity

$$N = |B|^2 = \lim_{t\to\infty}\left\langle \frac{P(t)^2}{2M} + \frac{M}{2}\omega^2 X(t)^2 \right\rangle/(\hbar\omega) \tag{37}$$

is the final energy of the oscillator measured in units of $\hbar\omega$. In a purely classical treatment the energy distribution is a single delta-function at $E_{\mathrm{osc}} = N\hbar\omega$.

A nice property of the *semiclassical approximation* is that from the ingredients of a purely classical calculation one can obtain a quantum mechanical distribution of the final state energies over the quantized energies E_n with a nonzero width. Then the quantity N is just the *average* number of excited phonons.

In principle, one can use (24) also to calculate the matrix elements starting from excited states. One may wonder, however, if this could be done with the same trajectory and hence the same B. In principle, one would have to start with a trajectory of a classically excited oscillator. The result would then depend on the phase of the oscillator coordinate and would eventually have to be averaged over the phases. Alternatively one could consider Ehrenfest's theorem for a moving excited oscillator wave function. Then for each excited state and given *total* energy, one would have a different trajectory. We are not aware of a systematic treatment of the semiclassical (coherent state) approximation along any of these alternatives.

Using different trajectories for different initial oscillator states $|m\rangle$ may lead to difficulties with symmetry properties of S following from the time reversal invariance. For a given total energy this symmetry leads to $P_{n,m} = P_{m,n}$. In the special case of $m = 0$ one can, therefore, calculate the transition probabilities $P_{0,\,\mathrm{m}}$ from an excited state $|m\rangle$ to the ground state directly from $P_{m,0}$ without changing the trajectory, i.e., by using the same B for both processes.

More generally, one can fulfill all symmetry properties by using the same B for all transitions. The trajectory which is used to calculate B can be taken as above with the oscillator initially at rest and the initial kinetic energy of the particle equal to the total energy E, but this condition can be varied in order to describe some dominant transitions optimally. In our example the one- and two-phonon transitions from the ground state are strong and should be accurately described.

C. Exponentiated Born Approximation. Finally, we come to the exponentiated Born approximation.[24,25] It is closely related to the FOA. The motion of the particle is treated separately from the oscillator in the sense of perturbation theory, but quantum mechanically. It is well-known that the quantum

mechanical matrix elements correspond to Fourier transforms of the corresponding classical variables. Hence, it is to be expected that the Fourier transform $F(\omega, E)$ in (21) corresponds to a quantum mechanical matrix element $\langle q_f|f|q_i\rangle$ of the force $f(z)$ (which becomes ω-dependent via total energy conservation).

To determine this matrix element, it is useful to consider matrix elements of (19) similar to the procedure used by Scarfone[8] in the derivation of the S-matrix for the FOM, however, generalized to the full S matrix. Since we want to determine only a single complex number, it is sufficient to consider only a single matrix element of (19). Let us consider the matrix element (in analogy to section III of ref 8)

$$S_{1,0} = {}_{\text{out}}\langle 1,q_f|0,q_i\rangle_{\text{in}} = {}_{\text{out}}\langle 0,q_f|b_{\text{out}}|0,q_i\rangle_{\text{in}} \tag{38}$$

To obtain the r.h.s of this expression we have made use of (19) and the fact that b_{in} applied to the "in" state, starting from the ground state, vanishes. Then, the integration over t in (19) yields $2\pi\hbar$ times the energy conserving delta-function which expresses the overall on-the-energy-shell character of the S-matrix element, and we have after dividing out this singular factor:

$$S_{1,0} = {}_{\text{out}}\langle 0,q_f|x_0 f|0,q_i\rangle_{\text{in}}/\hbar \tag{39}$$

where the force operator f is here taken in the Schrödinger picture.

Equation 39 is still rigorous. The *EBA* is obtained by adopting the perturbational approach in which the recoil term x in $f(z - x)$ of eq 19 is neglected. This means that in this approximation the correlation between the action of two successive $b^\dagger(t_1)$ and $b^\dagger(t_2)$ or $b(t_1)$ and $b(t_2)$ in the intermediate states is neglected. The matrix element (39) is then factorized as

$$S_{1,0} = {}_{\text{out}}\langle q_f|u_0 f(z)|q_i\rangle_{\text{in}} S_{0,0} \tag{40}$$

To indicate the analogy to the FOA, we use energy conservation

$$E = \frac{q_i^2}{2M} = \frac{q_f^2}{2M} + \hbar\omega = \text{constant} \tag{41}$$

to express the quantities $q_{i,f}$ in terms of E and ω and introduce the notation

$${}_{\text{out}}\langle q_f|f(z)|q_i\rangle_{\text{in}} = f(\omega,E) \tag{42}$$

The phase space displacement B in EBA then reads

$$B^{\text{EBA}} = \frac{x_0}{\hbar} f(\omega,E) = f(\omega,E)/(2M\hbar\omega)^{1/2} \tag{43}$$

in complete analogy with the FOA result (21). Expression (43) enables the calculation of the EBA mean number of emitted phonons

$$N^{\text{EBA}} = |B^{\text{EBA}}|^2 \tag{44}$$

and the corresponding Debye−Waller factor

$$|S_{0,0}^{\text{EBA}}|^2 = \mathrm{e}^{-N^{\text{EBA}}} = \exp[-|f(\omega,E)|^2/(2M\hbar\omega)] \tag{45}$$

Then, expressions (40)−(45) enable the construction of the EBA multiphonon scattering probabilities in the form

$$P_{n,0}^{\text{EBA}} = \mathrm{e}^{-N^{\text{EBA}}} \frac{(N^{\text{EBA}})^n}{n!} \tag{46}$$

which satisfy the unitarity condition (29). Here, in analogy to the trajectories of the semiclassical approximation, one could ask if for different transitions the different matrix elements should be considered. Again, the answer is that the symmetry and unitarity of $S_{n,m}$ is most easily ensured if the same B is taken for all the transitions.

The main difference between the FOA and the EBA is the fact that, due to the total energy conservation, the quantum on-the-energy-shell matrix element $f(\omega, E)$ vanishes below the threshold for one-phonon transitions (i.e., for $E < \hbar\omega$). As a consequence, the Debye−Waller factor $e^{-N^{\text{EBA}}}$ is unity below the threshold. Furthermore, the behavior of $f(\omega, E)$ near and above the threshold is $\propto\sqrt{p_f}$, leading to the threshold behavior $\propto(E - \hbar\omega)^{1/2}$ of the one-phonon transition probability $P_{1,0}$.

The two and higher order multi-phonon transition probabilities, $P_{n\geq 2,0}^{\text{EBA}}$, do not have the correct behavior below and just above the corresponding two and higher multi-phonon thresholds. The correct behavior could be (partly) achieved by modifying the energy dependence of higher order powers of the on-the-energy-shell first-order transition matrix element (42): the corresponding values of the n-phonon transition probabilities obtained from (46) may be put equal to zero by the constraint of total energy conservation. However, this would violate the unitarity of S^{EBA} and the corresponding transition probabilities given by eq 46 which sum up to unity. A hint as how $P_{n,0}^{\text{EBA}}$ could be put on the energy shell and the unitarity preserved is provided by a comparison of the FOA and the EBA transition probabilities below the 1-phonon threshold. Here we have $P_{1,0}^{\text{EBA}} = 0$ below threshold and $P_{0,0}^{\text{EBA}} = 1$, whereas in the FOA the one (zero) phonon contribution increases (decreases) continuously from 0 (1) onward. The EBA result can be approximated quite well (as we shall see) by (i) chopping off the 1-phonon contribution of the FOA below the 1-phonon threshold and (ii) adding such chopped off contribution to the 0-phonon transition probabilities. The physical argument (from the wave function point of view) is that below threshold the energy conservation does not allow a displacement of the incoming wave function in the asymptotic region. Above the threshold, however, an asymptotic displacement can occur and leads to a reduction of the 0-phonon contribution.

More generally, due to the total energy conservation, below the n-phonon threshold there can be no asymptotic displacement leading to n-phonon transitions. Above threshold this can happen and leads to a reduction of the $(n - 1)$-phonon transitions. This suggests the following prescription for improving the SEC and EBA: below the n-phonon threshold the n-phonon contributions should be subtracted from the respective $P_{n,0}$ (i.e. replaced by zero) and added to $P_{n-l,0}$ ($n > l \geq 1$), consistent with the total energy conservation.

IV. Comparison with Coupled Channel Approach

In the coupled channels (CC) approach, the wave function is expanded in oscillator eigenfunctions (channels). The Schrödinger equation then becomes a system of coupled 1D second order differential equations. If the potential is replaced by a stepwise constant potential, with sufficiently many steps to ensure a good representation of the actual $v(z)$, one can use the transfer matrix method to solve these equations. We work with local reflection (LORE) matrixes in order to avoid numerical instabilities due to closed channels. The LORE-matrixes (apart from normalization factors) approach the scattering matrixes $S_{n,m}$ asymptotically[39] and hence can be compared directly to the corresponding matrixes introduced above.

We use 100 to 200 equidistant steps of the potential between $z_i = -1.4$ Å and $z_f = 5.5$ Å, $N_v = 6$ channels and 600

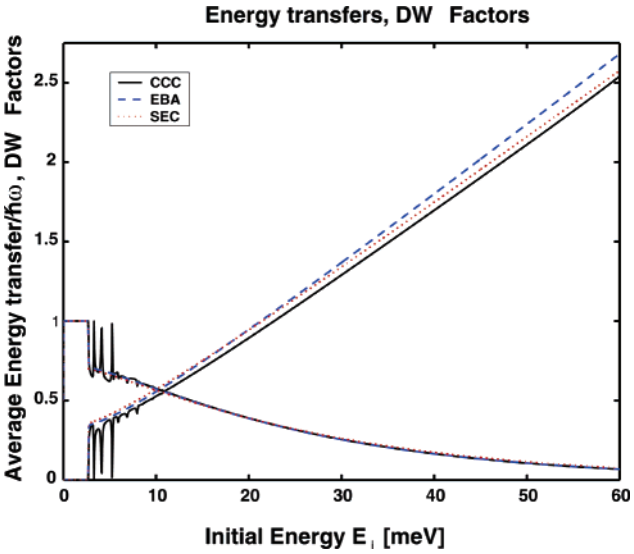

Figure 1. Comparison of the magnitudes of energy transfers (increasing at high energies) and Debye-Waller factors (decreasing at high energies) as calculated in the CCC, EBA, and SEC, and shown as functions of the initial kinetic energy E_i of the projectile measured in meV. At higher energy the excitation probabilities are dominated by 2 and 3 phonon processes. Note the pronounced low energy structure in the CC results which is absent in EBA and SEC. Note that at high energies the SEC agrees better with the CCC results than the EBA. This results from high order (i.e. multiphonon) recoil effects, which are not taken into account in the EBA.

equidistantly spaced energies between $E = 0$ meV and $E = 12$ or 60 meV. The small energy spacing is necessary to resolve the resonance structure at low energies showing up below 12 meV, in the larger energy interval 60 meV we did not care about the details of these structures. An increase to 300 steps and 8 channels leads only to negligible changes in the results.

In Figure 1, we compare the (average) energy transfer to the oscillator for initial ground states measured in units of $\hbar\omega$, viz.

$$E_{osc}/(\hbar\omega) = \sum_n nP_{n,0} = N = |B|^2 \qquad (47)$$

as obtained in the semiclassical approximation and the EBA, N_{SEC} and N_{EBA}, with the exact N_{CCC} of the coupled channel method.

Second, in Figure 2, we present the ground-state transition probabilities $P_{n,0} = |S_{n,0}|^2$, again calculated in the CC, EBA, and SEC approach as functions of the initial projectile energy. It turns out that at high incident energies (around 60 meV) 2- and 3-phonon processes dominate, leading to the average energy transfer of 2.7 phonons but there is also substantial 1-, 4-, and 5-phonon excitation. At low energies (below 10 meV), the average energy transfer is only around 0.5 phonons. Surprisingly enough, the resonance structure in this region contains strong 3- and 4-phonon contributions. It is also interesting to note that the resonances occur very strongly in the DWF. This means the 2-, 3-, and 4-phonon stimulated structure corresponds to an enhanced *elastic* scattering, and a corresponding suppression of inelastic 1-phonon scattering. This is just the opposite of the usual phonon stimulated inelastic processes. We consider the energy region of the resonances in more detail.

To interpret the resonance structure we consider the three bound states of the Morse potential and add to them all possible 1-, 2-, and 3-phonon excitation energies. This leads to four states below zero energy which do not participate in scattering.

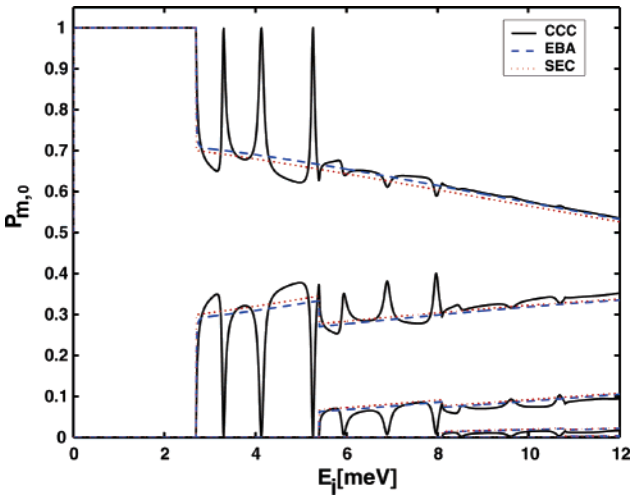

Figure 2. Comparison of the SEC, EBA, and CCC excitation probabilities $P_{m,0}$ for the first 5 vibrational levels (decreasing in intensity with increasing m) as functions of the initial projectile kinetic energy Ei measured in meV. Note the pronounced structure in the CCC results which is absent in EBA and SEC, but also in the CCC results of ref 37 because of the purely repulsive character of the projectile-oscillator interaction considered in that work. Between the 1- and 2-phonon threshold the agreement between approximate and exact results is greatly improved by the "chop-off" procedure described in the text.

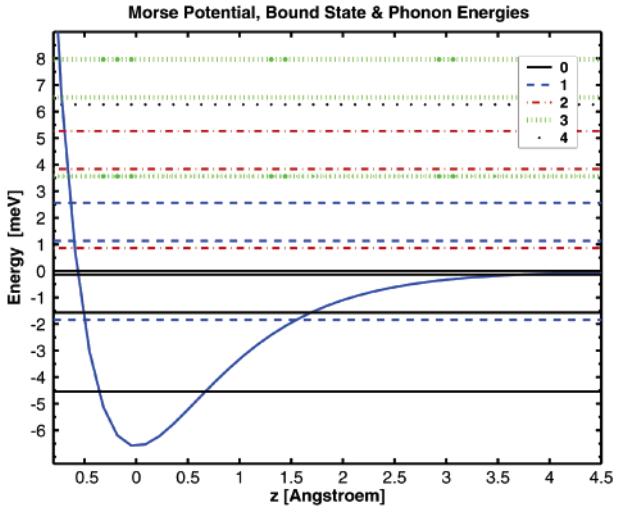

Figure 3. Morse potential together with its three bound states and all one- to three-phonon levels as well as the lowest four-phonon state.

Three of the remaining eight states are below the single-phonon threshold and lead only to a resonant change of the scattering phase $\delta(E_i) = -i\ \ln(S_{0,0})$ but do not influence the DWF. Then there are five more states above the threshold which then can lead to resonances in the scattering probabilities. A glance at Figure 2 shows that they give rise to six strong peaks (an apparent peak just above the two phonon threshold is only a threshold anomaly). Here the peak near 6 meV does not fit into our twelve level scheme. However, it vanishes in a four channel calculation and shows up only for five and more channels. From this, we conclude that it is a four-phonon state (over the ground state of the Morse potential).

In comparing the calculated levels with the energy scheme of Figure 3, one has to take into account that the zero-order levels in the potential $v(z)$ are perturbed by the coupling term $v(z - x) - v(z)$. The surprising result is *(i)* the strong two- to four-phonon resonances in a region where the *average* energy transfer is only of the order 0.5, and *(ii)* the fact that strong

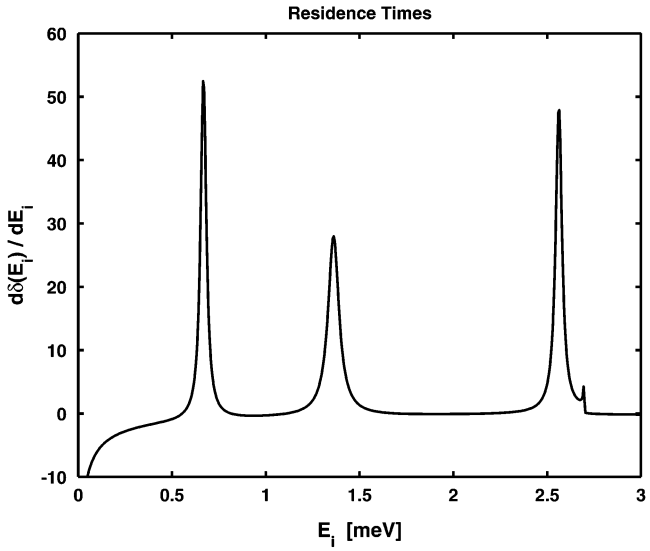

Figure 4. Residence time $d\delta(E_i)/dE_i$ as a function of incident projectile energy below the 1-phonon threshold.

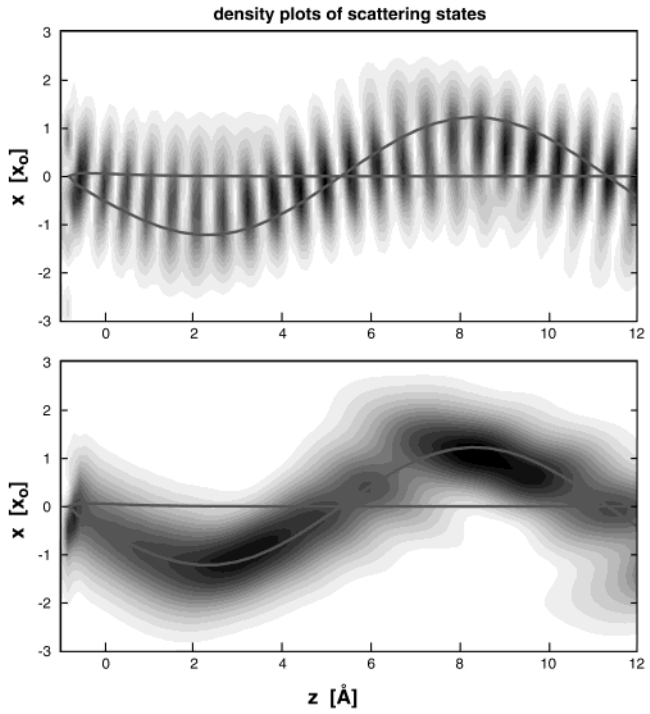

Figure 5. Density contours of the scattering wave function at 15 meV compared with classical trajectory. Upper part: Total wave function, lower part: scattered part of wave function.

excitation of phonons *inside the potential well* leads to an increase of the DWF, i.e., an increase of *elastic* scattering.

Concerning the three states within the "elastic scattering window" below the single phonon threshold we have determined the energy derivative of the elastic scattering phase $d\delta(E_i)/dE_i$ which is known to be the "residence time" (the delay time of a scattered wave packet as compared to the unperturbed wave).

The three peaks in this quantity may be identified with the corresponding three unperturbed levels in the energy diagram of Figure 3. A further interpretation of the results can be obtained from a consideration of the wave functions or the corresponding densities $|\langle x, z|0, q_i\rangle_{in}|^2$ respectively. Figure 5 shows, in the upper part, a contour plot of such a density for an energy of 15 meV, i.e., well above the resonance region. For comparison also the corresponding classical trajectory is shown.

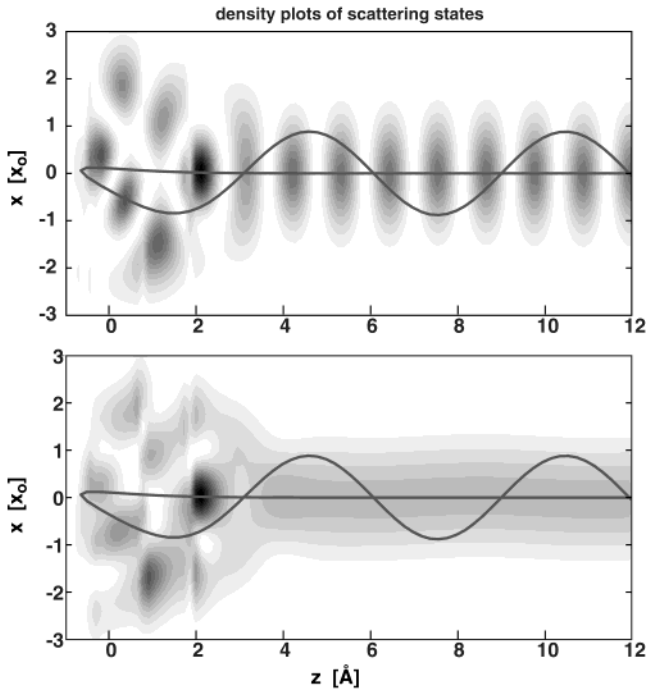

Figure 6. Density contours of the scattering wave function at 4.1325 meV compared with classical trajectory. Upper part: total wave function. Lower part: scattered part of wave function.

Obviously, the wave function follows in some way the trajectory but the correspondence is masked somewhat by the interference between the incoming and scattered parts of the wave function.

In the LORE procedure[39] these two parts can easily be calculated separately. The lower part of Figure 5 shows the density of the scattered part alone again compared to the classical trajectory. The correspondence is now clearly visible. Furthermore, one can see that the wave function is nicely coherent up to about 5 Å, a distance above which the potential becomes negligible. With increasing distance from this "scattering region" the spatial coherence gradually decreases. This is the result of "dephasing" of the components of the wave function with different oscillator energies. Since it occurs in the asymptotic regime, i.e., outside the scattering region, it has no influence on the energy distribution. The situation becomes drastically different at the resonance energies. We consider as an example the second resonance state above the one phonon threshold at an energy of 4.1325 meV. Figure 6 again shows density plots of the total and scattered wave function. Now the coherence is destroyed *inside* the potential well and retained outside.

Furthermore the wave function shows no oscillation in the x direction in the asymptotic region: The scattering is elastic. This is in contrast to the classical trajectory at the same energy which shows the semiclassical inelasticity which is slowly varying near energies around 4.1 meV.

Third, we consider more generally the excited-state transition probabilities $P_{n,m} = |S_{n,m}|^2$ for the first three excited states obtained from CC calculations. Figure 7 shows such excitation probabilities. The consideration of these probabilities is necessary for experiments at nonzero temperatures T_s since then the n-phonon excitation probabilities are given by[12]

$$P_n(T_s) = \sum_m P_{m+n,m} \exp(-\hbar\omega m/(kT_s))/Z \qquad (48)$$

where Z is the oscillator partition function. The DWF corresponds to $n = 0$. A glance at Figure 7 and eq 48 indicates that

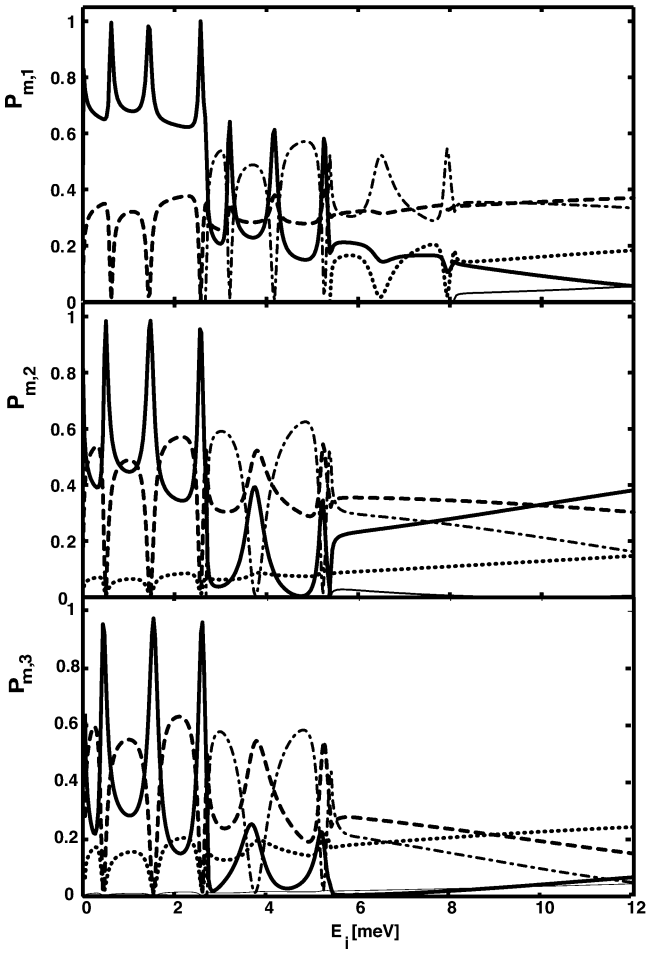

Figure 7. Phonon transition probabilities starting from excited initial states $m = 1, 2, 3$ as a function of incident *kinetic* energy E_i. Thick solid lines: Diagonal terms ($P_{m,m}$), dashed lines: 1phonon-down processes ($P_{m-1,m}$), dash-dotted lines: 1phonon-up process ($P_{m+1,m}$), dotted lines: 2phonon-up processes ($P_{m+2,m}$), thin solid lines: Other processes.

the dominant nonzero$-T_s$ effect is the occurrence of three additional peaks below the one-phonon threshold.

It is interesting to check the symmetry $P_{n,0} = P_{0,n}$ by comparing the results of Figures 2 and 7. (Note that the symmetry is valid for fixed *total* energy, whereas Figure 7 shows the results as function of the projectile *kinetic* energy.)

V. Discussion and Conclusions

We have considered the scattering of Helium atoms by dispersionless phonons and compared the results of two approximations, the semiclassical forced oscillator approximation (SEC) and the exponentiated Born approximation (EBA) with exact coupled channel calculations (CCC). We have calculated elastic and inelastic scattering cross sections, elastic scattering phase shifts, wave functions and classical trajectories.

The two approximations on the average, in particular at intermediate energies, agree quite well with the exact results. The threshold behavior near the n-phonon excitation energies is only given correctly near the 1-phonon energy in the EBA but can be approximately described in terms of a chop-off procedure with subsequent unitarizing. At high energies, SEC is better than the EBA because of the higher order recoil effects.

The main discrepancies occur at low energies. Here the exact results exhibit strong resonances which are absent in both approximations. The resonance energies are close to multi-phonon excitation energies on top of bound states of He-atoms in the attractive well. To observe such resonances, one has to go to sufficiently low energies, by considering low beam energies, nonzero scattering angles, and/or adsorbates with lower atomic mass than Xe and consequently higher ω. Elastic specular scattering then yields the DWF. In our calculation, the width of the resonances is only due to coupling to the entrance/exit channel. Additional broadening will occur by coupling to the substrate phonons and dispersion of the Einstein-modes. Experimentally both effects are known to be small. We therefore believe the resonances have a good chance to be observable.

The scattering wave functions (except near the resonances) are coherent states following classical trajectories. At resonance, the coherence is destroyed inside the attractive well. It will be interesting to generalize EBA to account for the resonances (for instance by considering the single particle Green's function, see ref 40) and to formulate a theory of sticking in terms of such a generalization.

Acknowledgment. This work was supported in part by the Bavarian-Croatian bilateral research project "Interaction of gases with surfaces".

References and Notes

(1) Jackson, J. M.; Mott, N. F. *Proc. R. Soc. (London)* **1932**, *A137*, 703. Lennard-Jones, J. E.; Strachan, C. *Proc. R. Soc.* **1935**, *A150*, 442. Strachan, C. *Proc. R. Soc.* **1935**, *A150*, 456. Lennard-Jones, J. E.; Devonshire, A. F. *Proc. R. Soc.* **1936**, *A156*, 29. Devonshire, A. F. *Proc. R. Soc.* **1937**, *A158*, 269. Lenard-Jones, J. E.; Devonshire, A. F. *Nature* **1936**, *137*, 1069. Devonshire, A. F. *Proc. R. Soc.* **1936**, *A156*, 37. Lennard-Jones, J. E.; Devonshire, A. F. *Proc. R. Soc.* **1937**, *A158*, 242. Lennard-Jones, J. E.; Devonshire, A. F. *Proc. R. Soc.* **1937**, *A158*, 253.

(2) Cabrera, N.; Celli, V.; Goodman, F. O.; Manson, J. R. *Surf. Sci.* **1970**, *19*, 67.

(3) Manson, J. R.; Celli, V. *Surf. Sci.* **1971**, *24*, 495.

(4) Goodman, F. O. *Surf. Sci.* **1971**, *24*, 667. *J. Chem. Phys.* **1971**, *55*, 5742.

(5) Armand, G. *J. Phys. (France)* **1989**, *50*, 1493 and references therein.

(6) Gol'dman, I. I.; Krivchenkov, V. D. *Problems in Quantum Mechanics*; Addison-Wesley: Reading, MA, 1961. Kogan, V. I.; Galitskiy, V. M. *Problems in Quantum Mechanics*; Prentice Hall: Englewood Cliffs, NJ, 1963.

(7) Fuller, R. W.; Harris, S. M.; Slaggie, E. L. *Am. J. Phys.* **1963**, *31*, 431.

(8) Scarfone, L. M. *Am. J. Phys.* **1964**, *32*, 158.

(9) Carruthers, P.; Nieto, M. M. *Am. J. Phys.* **1965**, *33*, 537 and references therein.

(10) Mahan, G. D. *Many-Particle Physics*; Plenum Press: New York, 1981.

(11) Gumhalter, B. *Phys. Rep.* **2001**, *351*, 1.

(12) Sunko, D. K.; Gumhalter, B. *Am. J. Phys.* **2004**, *72*, 231.

(13) Kaplan, J. I.; Drauglis, E. *Surf. Sci.* **1973**, *36*, 1.

(14) Burke, K.; Kohn, W. *Phys. Rev.* **1991**, *B43*, 2477.

(15) Schlichting, H.; Menzel, D.; Brunner, T.; Brenig, W.; Tully, J. C. *Phys. Rev. Lett.* **1988**, *60*, 2515.

(16) Brenig, W. *Z. Phys.* **1980**, *B 36*, 227. Böheim, J.; Brenig, W.; Stutzki, J.; *Z. Phys.* **1982**, *B 48*, 48; Erratum: *Z. Phys.* **1983**, *B 49*, 362. Brenig, W.; Russ, R. *Surf. Sci.* **1992**, *278*, 397.

(17) Garibaldi, U.; Levi, A. C.; Spadacini, R.; Tommei, G. E. *J. Appl. Phys.* **1974**, *Suppl. 2, Pt.2*; *Surf. Sci.* **1975**, *48*, 649.

(18) Levi, A. C. *Nuovo Cimento* **1979**, *54B*, 357.

(19) Bortolani, V.; Levi, A. C. *Atom−Surface Scattering Theory*, La Rivista del Nuovo Cimento 9/11(1986)1.

(20) Bertino, M.; Ellis, J.; Hofmann, F.; Toennies, J. P.; Manson, J. R. *Phys. Rev. Lett.* **1994**, *73*, 605.

(21) Bracco, G.; Cantini, P.; Glanchant, A.; Tatarek, R. *Surf. Sci.* **1983**, *125*, L81.

(22) Škorupka, C. W.; Manson, J. R. *Phys. Rev. B* **1990**, *41*, 9783.

(23) Šiber, A.; Gumhalter, B. *Surf. Sci.* **2003**, *529*, L269.

(24) Brenig, W. *Z. Phys.* **1979**, *B 36*, 81; Böheim, J.; Brenig, W. *Z. Phys.* **1981**, *B 41*, 243.

(25) Burke, K.; Gumhalter, B.; Langreth, D. C. *Phys. Rev.* **1993**, *B47*, 12852; Gumhalter, B.; Burke, K.; Langreth, D. C. *Surf. Rev. Lett.* **1994**, *1*, 133.

(26) Bilić, A.; Gumhalter, B. *Phys. Rev. B* **1995**, *16*, 12307.

(27) Müller-Hartmann, E.; Ramakrishnan, T. V.; Toulouse, G. *Phys. Rev. B* **1971**, *3*, 1102.
(28) Schlichting, H.; Menzel, D.; Brunner, T.; Brenig, W. *J. Chem. Phys.* **1992**, *97*, 4453.
(29) Brunner, T.; Brenig, W. *Surf. Sci.* **1993**, *291*, 192.
(30) Braun, J.; Fuhrmann, D.; Šiber, A.; Gumhalter, B.; Wöll, Ch. *Phys. Rev. Lett.* **1998**, *80*, 125. Šiber, A.; Gumhalter, B.; Braun, J.; Graham, A. P.; Bertino, M.; Toennies, J. P.; Fuhrmann, D.; Wöll, Ch. *Phys. Rev. B* **1999**, *59*, 5898.
(31) Gumhalter, B.; Šiber, A.; Toennies, J. P. *Phys. Rev. Lett.* **1999**, *83*, 1375.
(32) Šiber, A.; Gumhalter, B.; Wöll, Ch. *J. Phys. Cond. Matter* **2002**, *14*, 5193.
(33) Boas, Ch.; Kunat, M.; Burghaus, U.; Gumhalter, B.; Wöll, Ch. *Phys. Rev. B* **2003**, *68*, 075403 and references therein.
(34) Brenig, W.; Brako, R.; Hilf, M. *Z. Phys. Chem.* **1996**, *197*, 237. Brenig, W.; Hilf, M.; Brako, R. *Surf. Sci.* **2000**, *469*, 105.
(35) Brenig, W.; Hilf, M. F. *J. Phys. C* **2001**, *13*, R61.
(36) Kasai, H.; Brenig, W. *Z. Phys.* **1985**, *B 59*, 429.
(37) Šiber, A.; Gumhalter, B. *Phys. Rev. Lett.* **2003**, *90*, 126103.
(38) Brenig, W. *Phys. Rev.* **1997-I**, *B 55*, 10119.
(39) Brenig, W.; Brunner, T.; Gross, A.; Russ, R. *Z. Phys.* **1993**, *B93*, 91; Brenig, W.; Russ, R. *Surf. Sci.* **1994**, *315*, 195; Brenig, W.; Gross, A.; Russ, R. *Z. Phys.* **1995**, *B97*, 311.
(40) Böheim, J.; Brenig, W. *Z. Phys.* **1982**, *B48*, 43.